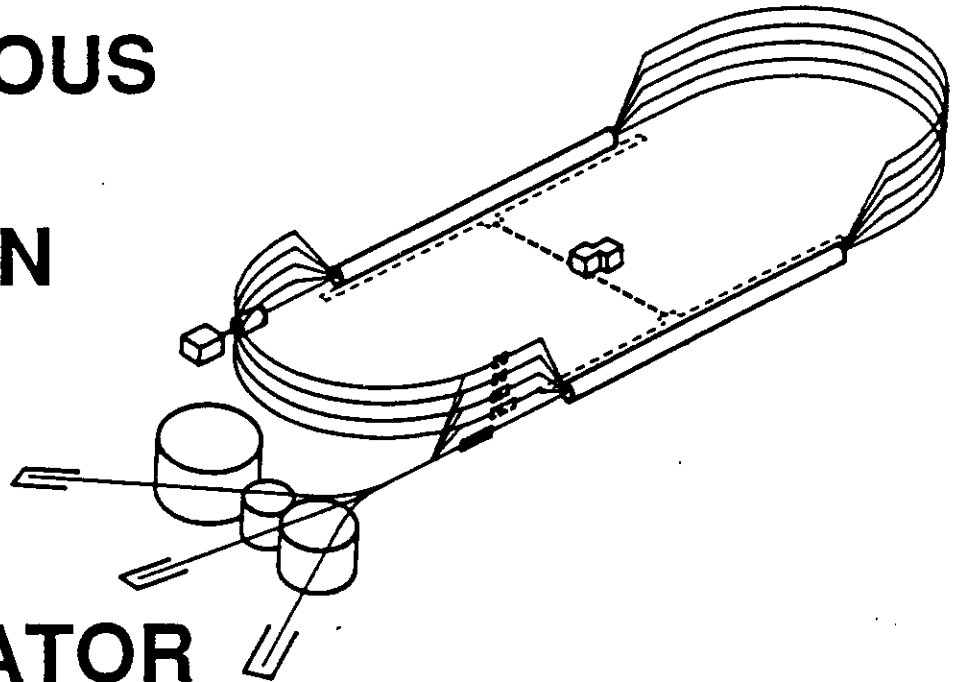


**POLARIZED STRUCTURE FUNCTIONS of the NUCLEON  
in the RESONANCE REGION**

V.D.Burkert  
12000 Jefferson Avenue, Newport News,  
Virginia 23606, USA

\*Presented at the Symposium on Polarized Structure Functions  
Yale University, New Haven, January 5-6, 1994

**C**ONTINUOUS  
**E**LECTRON  
**B**EAM  
**A**CCCELERATOR  
**F**ACILITY



**SURA** Southeastern Universities Research Association

**CEBAF**

The Continuous Electron Beam Accelerator Facility

Newport News, Virginia

Copies available from:

Library  
CEBAF  
12000 Jefferson Avenue  
Newport News  
Virginia 23606

The Southeastern Universities Research Association (SURA) operates the Continuous Electron Beam Accelerator Facility for the United States Department of Energy under contract DE-AC05-84ER40150.

#### DISCLAIMER

This report was prepared as an account of work sponsored by the United States government. Neither the United States nor the United States Department of Energy, nor any of their employees, makes any warranty, express or implied, or assumes any legal liability or responsibility for the accuracy, completeness, or usefulness of any information, apparatus, product, or process disclosed, or represents that its use would not infringe privately owned rights. Reference herein to any specific commercial product, process, or service by trade name, mark, manufacturer, or otherwise, does not necessarily constitute or imply its endorsement, recommendation, or favoring by the United States government or any agency thereof. The views and opinions of authors expressed herein do not necessarily state or reflect those of the United States government or any agency thereof.

# Polarized Structure Functions of the Nucleon in the Resonance Region

Volker D. Burkert

CEBAF, 12000 Jefferson Avenue, Newport News,  
Virginia 23606, USA

## ABSTRACT

Aspects of the spin structure functions of proton and neutrons at low momentum transfer  $Q^2$  and energy transfer  $\nu$ , i.e. in the region of the nucleon resonances are discussed. Experiments to measure  $A_1^p$ ,  $A_2^p$  and  $A_1^n$  structure functions at CEBAF in a  $Q^2$  range from 0.15 to 2.0  $\text{GeV}^2$ , and a  $W$  range from threshold to 2.2  $\text{GeV}$  are presented.

## 1. Introduction

The results of the EMC measurements<sup>1</sup> on the polarized proton structure functions have prompted numerous speculations about whether or not in the deep-inelastic region the spin of the proton is carried by the quarks. Recent results from the CERN Spin Muon collaboration (SMC)<sup>2</sup> and SLAC experiment E142<sup>3</sup> on the neutron polarized structure functions added to these speculations as in one interpretation the neutron spin is not carried by quarks either, whereas in another interpretation, the (fundamental) Björken sum rule<sup>4</sup> would be violated while leaving the (less fundamental) Ellis-Jaffe sum rule<sup>5</sup> for the neutron intact. It is worth noting that the experiments on the neutron use data sets with  $Q^2$  as low as 1  $\text{GeV}^2$ . While such low  $Q^2$  values have been used in the analysis of unpolarized lepton scattering there is a lack of convincing evidence that polarized structure functions exhibit true scaling behavior at such low  $Q^2$ . Moreover, the  $W$  range used in these analyses ( $W \geq 2 \text{ GeV}$ ) may overlap part of the resonance region. Resonant states have been observed for masses up to 2.8  $\text{GeV}/c^2$  and many more states are predicted to exist in the mass region above 2.0  $\text{GeV}$ . This raises the question what their contributions are to the spin sum rules and how to correct for them when interpreting the measurements in terms of total spin carried by quarks. As the conclusion about the spin of the proton not being carried by quarks rests on relatively small differences between theoretical predictions and the data it is important to study such contributions before far-reaching conclusions about the origin of the nucleon spin may be drawn.

However, studies of the spin structure function of the nucleon in the resonance region and at low  $\nu$  are interesting in their own right. The study of the non-perturbative regime of the strong interaction is one of the main motivations for the construction of continuous wave electron accelerators at various locations around the

world. CEBAF, in particular, with its initial maximum energy of 4 GeV should play an important role in unravelling the internal structure of the light quark baryons in this regime.

One of the major programs at CEBAF is the study of excited states of the proton and neutron, and the measurement of their transition formfactors from the ground state nucleon.<sup>27</sup> The formfactors, or helicity amplitudes contain information on both the internal spatial structure as well as the spin structure of the transition. The expected accuracy and completeness of the experimental data should allow for order of magnitudes of improvements on the empirical information about the known states, and should generate significant information about predicted, yet undiscovered states.

Microscopic models of the nucleon structure, such as relativized versions of the quark model, bag models, Skyrme models, QCD sum rules, and others may be tested in detail against these results. Significant improvements of our understanding of the strong interaction force in the non-perturbative regime will hopefully result from this effort.

The nucleon is likely more complex than the simple constituent quark picture suggests. Gluonic excitations, or hybrids, may play an active role in spectroscopy, and pionic contributions may be important at small momentum transfers:

$$|N \rangle = \alpha |q^3 \rangle + \beta |q^3 G \rangle + \gamma |q^3 (q\bar{q}) \rangle + \dots$$

Understanding the relative importance of these contributions is obviously important for a detailed understanding of the nucleon structure. In fact, while gluonic excitations have been predicted by QCD inspired models, solid evidence for such states is still lacking. From a comparison with the quark model we can learn whether the strength of the  $|q^3 \rangle$  states can exhaust the full resonant strength of the spin integrals. If this were the case, there would be little room for gluonic or other states. The opposite, of course, is also correct, a lack of 3-quark strength in the spin integral would provide evidence for non-quark contributions.

Another possibility is that most of the proton spin missing in deep inelastic scattering resides in orbital angular momentum contributions. Such contributions are necessarily associated with extended objects and therefore cannot be probed in deep inelastic scattering, but they may be accessible at lower energies and momentum transfers. The low  $Q^2$ ,  $\nu$  region may therefore contain significant information about the spin structure of the nucleon.

Finally, measurement of the polarization asymmetries at low  $Q^2$  and  $\nu$  will provide constraint to models describing the  $Q^2$  evolution of the polarized structure functions in the deep inelastic regime.

## 2. Polarized Structure Functions of the Nucleon

The spin-structure of the nucleon is usually discussed in relation to the deep-inelastic polarized structure functions  $g_1(x)$ . In the kinematical regime of resonances and low  $Q^2$  use of total helicity 1/2 and 3/2 photon-nucleon absorption cross sections is more convenient. If beam and target are longitudinally polarized, the double

polarized inclusive electron scattering cross section may be written as:

$$\frac{d\sigma}{d\Omega dE'} = \Gamma_T \{ \sigma_T + \epsilon \sigma_L \pm \sqrt{1 - \epsilon^2} \cos \psi \sigma_T A_1 \pm \sqrt{2\epsilon(1 - \epsilon)} \sin \psi \sigma_T A_2 \} \quad (1)$$

where  $\psi$  is the angle between  $\vec{q}$  and the target polarization vector,  $\sigma_T$  and  $\sigma_L$  are the transverse and longitudinal total photon absorption cross section, and the sign  $\pm$  is related to the sign of the product of beam and target polarization (assumed to be unity).  $A_1$  and  $A_2$  are the polarized asymmetries:

$$A_1 = \frac{\sigma_{1/2}^T - \sigma_{3/2}^T}{\sigma_{1/2}^T + \sigma_{3/2}^T} \quad (2)$$

$$A_2 = \frac{\sigma^{TL}}{\sigma_{1/2}^T + \sigma_{3/2}^T} \quad (3)$$

where  $\sigma_{1/2}^T(Q^2, \nu)$  and  $\sigma_{3/2}^T(Q^2, \nu)$  are the transverse total absorption cross sections for total helicity  $\lambda_{\gamma N} = 1/2$  and  $\lambda_{\gamma N} = 3/2$ , respectively.  $A_1$  is limited to:

$$-1 \leq A_1 \leq +1 \quad ,$$

and  $A_2$  is a transverse-longitudinal interference term with an upper bound of:

$$A_2 \leq \sqrt{\frac{\sigma_L}{\sigma_T}} \quad (4)$$

At  $Q^2 = 0$ , the sum rule by Gerasimov,<sup>8</sup> and Drell and Hearn<sup>9</sup> (GDH) relates the difference in the total photoabsorption cross section on nucleons for  $\lambda_{\gamma N} = 1/2$  and  $\lambda_{\gamma N} = 3/2$  to the anomalous magnetic moment of the target nucleon.

$$\Gamma^{GDH} = \frac{M^2}{8\pi^2\alpha} \int_{\nu_{thr}}^{\infty} \frac{d\nu}{\nu} (\sigma_{1/2}^T(\nu) - \sigma_{3/2}^T(\nu)) = -\frac{1}{4}\kappa^2 \quad (5)$$

In the deep inelastic regime the first moment of the spin structure function is given by:

$$\begin{aligned} \Gamma_1(Q^2) &= \int_0^1 A_1(x, Q^2) \cdot F_1(x, Q^2) dx \\ &= \frac{Q^2}{16\pi^2\alpha} \int_{\nu_{thr}}^{\infty} (1-x) (\sigma_{1/2}^T(\nu, Q^2) - \sigma_{3/2}^T(\nu, Q^2)) \frac{d\nu}{\nu} \\ &\longrightarrow \frac{Q^2}{16\pi^2\alpha} \int_{\nu_{thr}}^{\infty} (\sigma_{1/2}^T(\nu, Q^2) - \sigma_{3/2}^T(\nu, Q^2)) \frac{d\nu}{\nu} \quad , \quad (Q^2 \rightarrow 0) \quad (6) \end{aligned}$$

The slope of  $\Gamma_1(Q^2)$  at  $Q^2 = 0$  is thus determined by the GDH sum rule (eqn.(5)).

### 3. Polarized Structure Functions and Spin Sum Rules at low $Q^2$ .

Assuming scaling behavior the EMC results can be extrapolated to lower  $Q^2$

$$I_p(Q^2) = \frac{2M_p^2}{Q^2} \Gamma_p^{EMC} \simeq \frac{0.222 \pm 0.018 \pm 0.026}{Q^2} \quad (7)$$

where QCD corrections have been neglected.

From the GDH sum rule one expects  $I_p(0)$  to be large and negative, whereas the EMC data yield a positive  $I_p(Q^2)$ . In order to reconcile the GDH sum rule with the EMC results, dramatic changes in the helicity structure must occur when going from  $Q^2 = 0$  to finite values of  $Q^2$ . In an analysis of photoproduction data by Karliner<sup>10</sup> and recently by Workman and Arndt<sup>11</sup> for energies up to  $E_\gamma = 1.7$  GeV single pion production contributions were found to nearly saturate the sum rule. The analysis of electroproduction data by Burkert and Li<sup>12,13</sup> including resonant channels as well as non-resonant single pion Born terms showed that contributions of the  $\Delta(1232)$  to  $I_p(Q^2)$  are dominant at small  $Q^2$ , and contributions from other resonances become significant with increasing  $Q^2$ , causing  $I_p(Q^2)$  to change its sign at  $Q^2$  between 0.5 to 1.0 GeV<sup>2</sup>. Anselmino et al.<sup>14</sup> attempted to connect the GDH sum rule with the

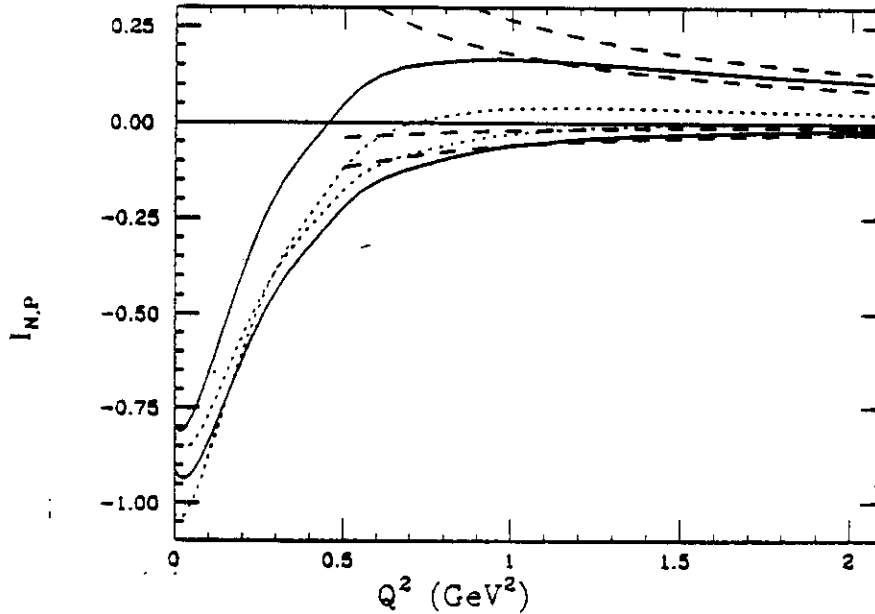
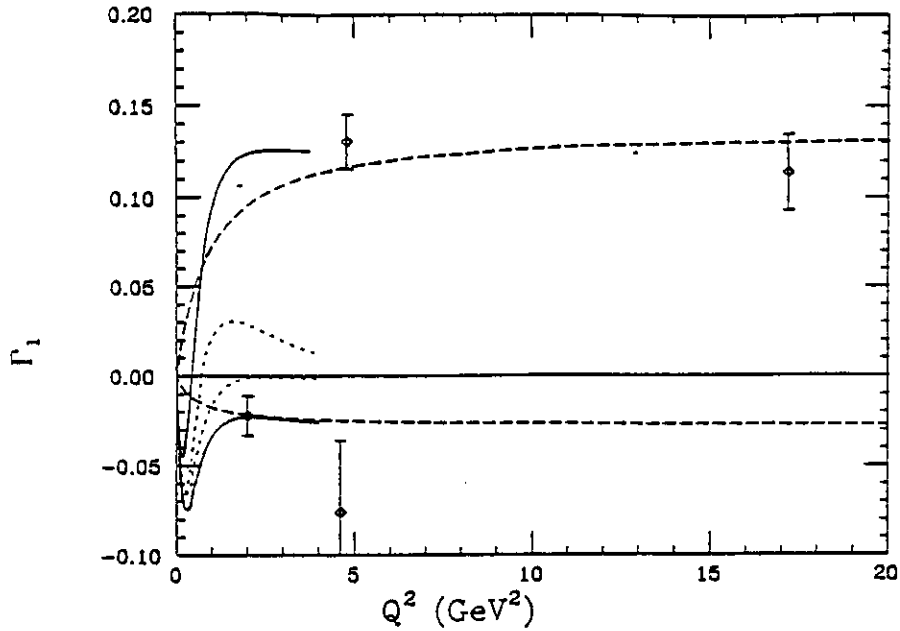


Figure 1: The integral  $I_{p,n}(Q^2)$ . The short dashed lines represent resonance contributions for proton (sign changing curve) and neutron, respectively. The solid lines include VDM contributions and are normalized to the GDH value at the photon point and to reproduce the EMC data on the proton, and the E142 data on the neutron, respectively. The dashed lines represent the extrapolated EMC results for protons (positive value), and the E142 results for neutrons (negative value), respectively.



**Figure 2:**  $\Gamma_{p,n}(Q^2)$ . Short dashed lines include resonances only,<sup>12</sup> solid lines - model by Burkert and Ioffe.<sup>15,16</sup> The lines with positive values at high  $Q^2$  are for protons, the lines with negative values are for neutrons. Data from EMC, E142, and SMC.

Ellis-Jaffe sum rule in the deep inelastic region using the vector dominance model analogy. The resulting strong  $Q^2$  dependence was found to be in disagreement with the EMC data. Burkert and Ioffe<sup>15,16</sup> extended this model to account for the resonance contributions obtained in<sup>12</sup>. The following expression is obtained:

$$I_{p,n}(Q^2) = \sum I_{p,n}^{Res}(Q^2) + 2M_p^2 \Gamma_{p,n}^{as} \left[ \frac{1}{Q^2 + m_p^2} - \frac{c_{p,n} m_p^2}{(Q^2 + m_p^2)^2} \right] \quad (8)$$

The parameters  $c_{p,n}$  are fixed by requiring  $I_{p,n}(0) = I_{p,n}^{GDH}$ . For the proton, the model is constraint to reproduce the EMC results at  $Q^2 = 10.7 \text{ GeV}^2$ , and for the neutron the E142 data at  $Q^2 = 2 \text{ GeV}^2$  are used. The model predicts significant high twist contributions at  $Q^2 \leq 4 \text{ GeV}^2$  (Fig. 2). Resonance contributions are significant  $Q^2 \leq 3 \text{ GeV}^2$ . Unfortunately, for  $Q^2 > 3 \text{ GeV}^2$  resonance excitations have not been measured, however, assuming a smooth falloff for the resonance contributions with  $Q^2$ , an approximate scaling behavior is predicted for  $Q^2 > 2 \text{ GeV}^2$ . In reference<sup>16</sup> the effect of such 'higher twist' contributions on the interpretation of the results of the EMC, E142, and SMC data are discussed, with the following results:

- (1) The spin fraction carried by the quarks in the proton is:

$$\Sigma_p = 0.28 \pm 0.17 ,$$

and in the neutron:

$$\Sigma_n = 0.53 \pm 0.14 .$$

(2) The spin fraction carried by strange quarks in the proton is:

$$\Delta s_p = -0.10 \pm 0.06 ,$$

and in the neutron:

$$\Delta s_n = -0.02 \pm 0.05 .$$

(3) The asymptotic proton-neutron difference

$$\Gamma_p^{as} - \Gamma_n^{as} = 0.165 \pm 0.024$$

is consistent with the Bjorken sum rule:

$$\Gamma_p - \Gamma_n = 0.186 \pm 0.003 .$$

The GDH integral for the neutron is of special interest at low  $Q^2$  for testing predictions of the quark model. In the  $SU(6) \otimes O(3)$  basis the GDH sum rule obtains contributions from the  $\gamma N \Delta(1232)$  transition only<sup>17,18</sup>:

$$I_n^{GDH}(Q^2) = I_n^{\Delta(1232)}(Q^2)$$

This prediction is based on the symmetry properties of the quark model; a deviation would indicate a breaking of the  $SU(6) \otimes O(3)$  symmetry and demonstrate the limitations of the nonrelativistic quark model. Resonance contributions to the GDH sum rule using the quark model have been discussed in detail by D. Drechsel and M. Giannini.<sup>28</sup>

The proton-neutron difference  $\Delta I_{pn}(Q^2)$  as a function of  $Q^2$  allows study of the transition from the Bjorken sum rule, which is expected to be valid in the deep inelastic region only, to the GDH sum rule at  $Q^2 = 0$ . In  $\Delta I_{pn}$  the dominant  $\Delta(1232)$  contribution is absent, such a measurement will hence be sensitive to isospin 1/2 resonance contributions, especially to the lowest mass state  $P_{11}(1440)$ . The 3-quark nature of this state has been disputed for some time. Calculations of transition form factors assuming it is a gluonic excitation<sup>20</sup> of the nucleon rather than a radial 3-quark excitation give better agreement with the experimental amplitudes. As shown in Fig. 3, measurements of  $\Delta I_{pn}$  are sensitive to the QCD structure of this state. The GDH value is  $\Delta I_{pn}(0) = +0.114$ . The analysis<sup>11</sup> of single pion photoproduction data is consistent with the analysis of electroproduction data<sup>12,13</sup> (Fig. 3) extrapolated to the photon point. Both analyses indicate a significant discrepancy with the GDH sum rule. However, this discrepancy may just be due to the limited kinematical range included in the analyses. Also, electroproduction data on neutrons are sparse, and the analysis has to rely largely on single quark transition symmetry arguments to determine the amplitudes for many of the higher mass states.

A violation of the GDH sum rule would be a significant finding. In recent theoretical work on extended current algebra<sup>21</sup> it is suggested that the GDH sum rule needs to be extended. Interestingly enough, the discrepancy observed in the empirical analyses is qualitatively consistent with this prediction. However, it is possible that contributions from the high energy region, or other non-resonant contributions the observed resonance contributions, account for the missing strength in the sum rule.

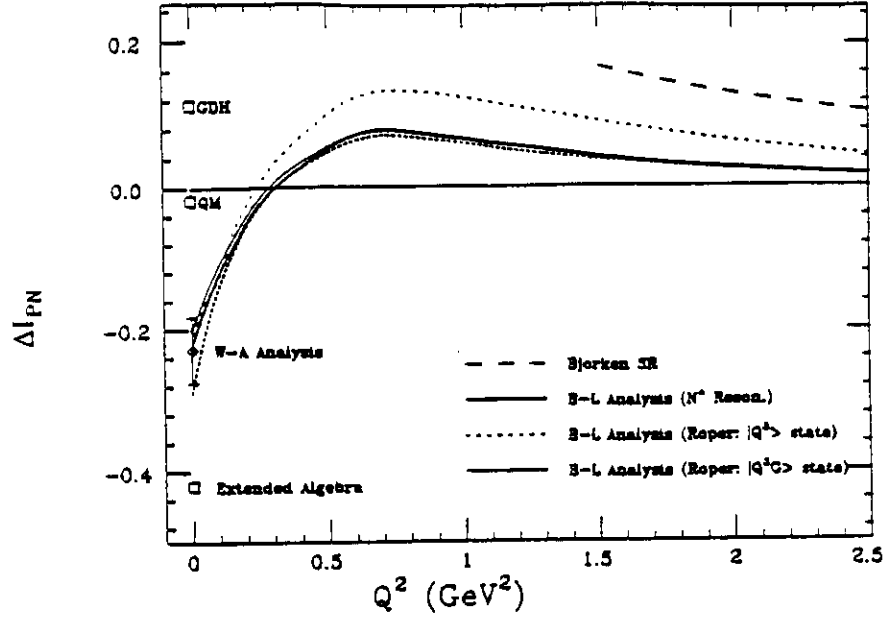


**Figure 3:** Result of the analysis of electroproduction of baryon resonances for the proton - neutron difference if only resonances are included using the AO code.<sup>19</sup> The  $P_{11}(1440)$  is assumed to be a  $(q^3)$  state in the nonrelativistic quark model (dashed-dotted), or as a  $(q^3G)$  hybrid state<sup>20</sup> (solid), QM denotes the quark model point, where photocoupling amplitudes of S. Capstick<sup>29</sup> have been used. Also shown is a proposed extension of the GDH sum rule using 'extended current algebra'.<sup>21</sup>

#### 4. Inclusive Polarized Electron Scattering Experiments at CEBAF

Experiment 91-023<sup>22</sup> will use the CEBAF Large Acceptance Spectrometer<sup>24</sup> to measure the asymmetries  $A_1^p(Q^2, \nu)$ , and  $A_2^p(Q^2, \nu)$  on the proton. The experimental arrangement is shown in Fig. 4. The  $^{15}\text{NH}_3$  target will be polarized along the beam axis. In order to separate  $A_1$  and  $A_2$  the experimental asymmetry

$$A \equiv \frac{\frac{d\sigma(\uparrow\uparrow)}{d\Omega dE'} - \frac{d\sigma(\uparrow\downarrow)}{d\Omega dE'}}{\frac{d\sigma(\uparrow\uparrow)}{d\Omega dE'} + \frac{d\sigma(\uparrow\downarrow)}{d\Omega dE'}} = P_e \cdot P_p \cdot D[A_1(Q^2, \nu) + \eta A_2(Q^2, \nu)] \quad (9)$$

$$D = \frac{\sqrt{1 - \epsilon^2} \cos \psi}{1 + \epsilon R}; \quad \eta = \sqrt{\frac{2\epsilon}{1 + \epsilon}} \tan \psi$$

will be measured at fixed  $Q^2$  and  $W$  but at different beam energies, giving different values for  $\eta$ .  $\psi$  is the angle between the polarization axis and  $\vec{q}$ . The experiment will measure the angular range for about  $13^\circ$  to  $48^\circ$  over most of the azimuthal angle range simultaneously. The solid angle covered is  $\Delta\Omega = 1.2$  sr. In the asymmetry, many systematic uncertainties, e.g. due to limited knowledge of the acceptance, will cancel.

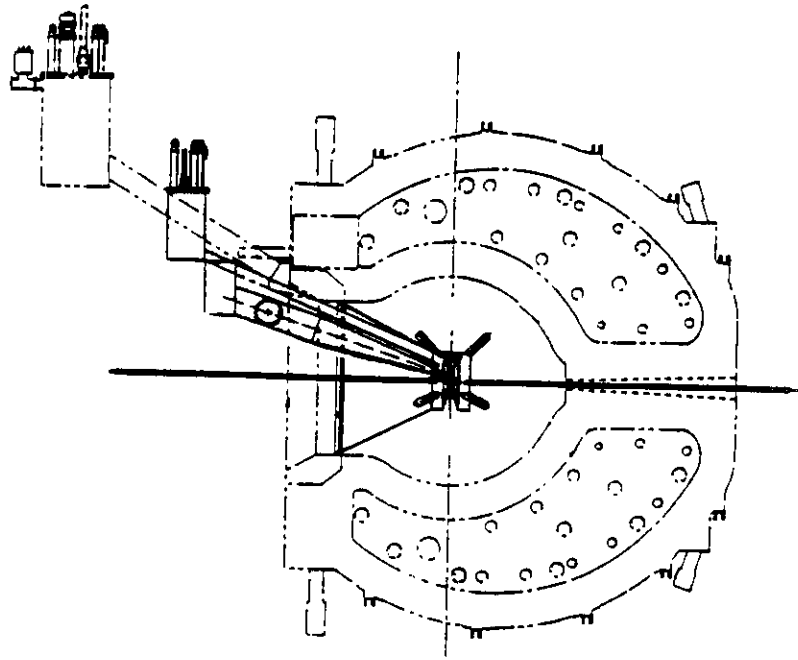


Figure 4: Experimental arrangement of the CEBAF experiment 91-023. The target is polarized parallel or anti-parallel to the beam axis.

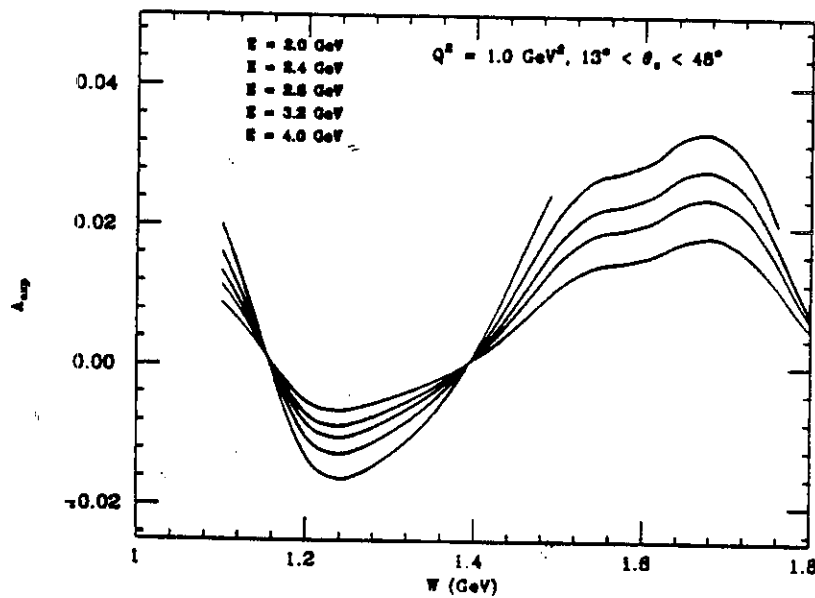


Figure 5: Expected experimental asymmetries for different beam energies but fixed  $Q^2$  and  $W$ . A fit of eqn.(9) to  $A$  at different energies allows the separation of  $A_1$  and  $A_2$ .

Systematic uncertainty due to the limited knowledge of beam and target polarization will be greatly reduced by measuring the elastic asymmetry

$$A_{ep} = P_e \cdot P_p \cdot f(G_E/G_M), \quad (10)$$

simultaneously.  $A_{ep}$  is a function of the ratio of electric and magnetic form factors, and the product of beam and target polarization. Since the form factors at small  $Q^2$  are known very accurately,  $P_e \cdot P_p$  can be determined to  $\delta(P_e \cdot P_p) \leq 0.01$ .

Fig. 6 shows expected experimental asymmetries for different beam energies. A fit of eqn(8) at fixed  $Q^2$  and  $W$  will allow the determination of  $A_1$  and  $A_2$ , separately. Expected error bars for the asymmetries are shown in Fig. 6, where data previously measured by a SLAC/Yale experiment at  $Q^2 = 0.5 \text{ GeV}^2$  are included for comparison. Asymmetries for 10 values of  $Q^2$  between  $0.15 \text{ GeV}^2$  and  $2 \text{ GeV}^2$  will be measured. In case  $A_2$  is known from some other source, e.g. from an analysis of unpolarized pion electroproduction data,  $A_1$  can be determined with considerably reduced error bars. The integral

$$I_p(Q^2) = \int_{\nu_{thr}}^{\nu(W \leq 2 \text{ GeV})} 2\sigma_T A_1 \frac{d\nu}{\nu} \quad (11)$$

will be determined with statistical errors as shown in Fig. 7.

Experiment 93-009<sup>25</sup> will measure the low  $Q^2$  behavior of  $I_n(Q^2)$  using a  $^{15}\text{N}\bar{D}_3$  target. The two experiments combined will allow extraction of the neutron GDH sum rule as well as the proton-neutron difference  $\Delta I_{pn}$ . Calculations using the AO code<sup>19</sup> show that for the neutron,  $A_2^n$  may be small, and one may extract  $A_1^n$  from eqn. (8) assuming  $A_2^n = 0$ . Fig. 8 shows the expected errors for the experimental asymmetry  $(A/D)\sigma_T$  on the neutron. Obviously, a very significant determination of  $\Delta I_{pn}(Q^2)$  will be possible (Fig. 9).

## 5. Exclusive Polarized Proton Asymmetries

Experiment 93-036<sup>26</sup> will measure polarization observables in single pion production. This experiment, in conjunction with the unpolarized experiments of the  $N^*$  program<sup>27</sup> will allow to isolate helicity transition amplitudes  $A_{1/2}$ ,  $A_{3/2}$  for individual resonances throughout the entire resonance region. The  $Q^2$  dependence of  $A_{1/2}$ ,  $A_{3/2}$  is sensitive to the QCD structure of resonant states. As already mentioned, the transverse  $A_{1/2}(Q^2)$  and the longitudinal  $S_{1/2}(Q^2)$  amplitudes for the  $P_{11}(1440)$  are very sensitive to the internal quark-gluon structure: ( $q^3$ ) state versus ( $q^3G$ ) state. As an illustrative example Fig. 10 shows first moments of the polarized target asymmetries for various models of the structure of the  $P_{11}(1440)$ . Measurement of  $A_{1/2}$ ,  $A_{3/2}$  for states with  $J \geq 3/2$  will allow the determination of helicity asymmetries:

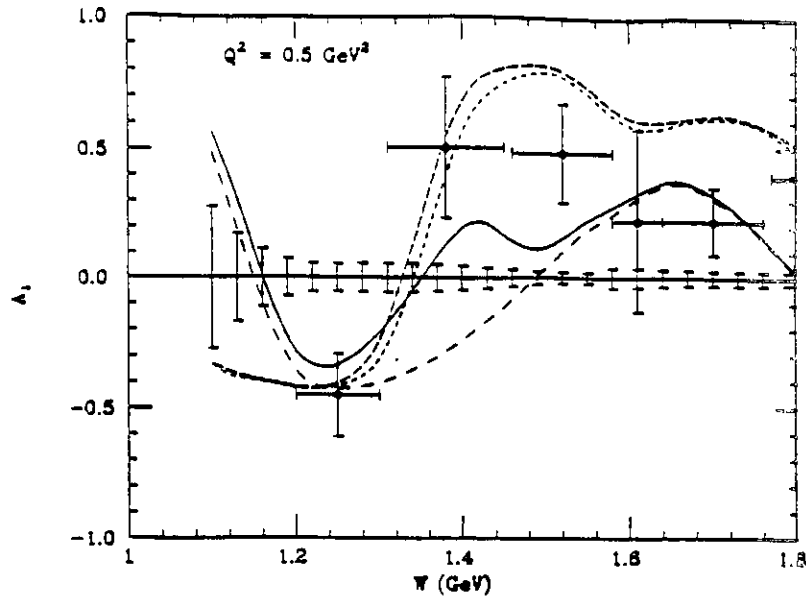


Figure 6: Expected statistical errors in experiment 91-023<sup>22</sup> for asymmetry  $A_1(Q^2, W)$  compared with SLAC/Yale data <sup>23</sup>

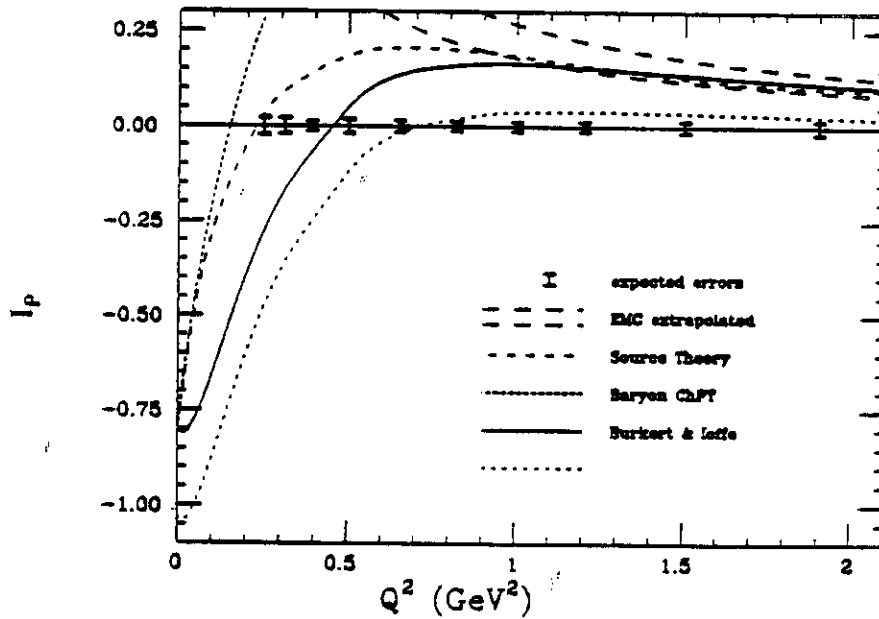


Figure 7: Expected errors for  $I_p(Q^2)$  from experiment 91-023<sup>22</sup> in comparison to model calculations: short dashes - chiral perturbation theory,<sup>31</sup> long dashes - source theory,<sup>30</sup> dotted - resonance contributions,<sup>12,13</sup> solid - resonances + vector meson dominance model<sup>15,16</sup>

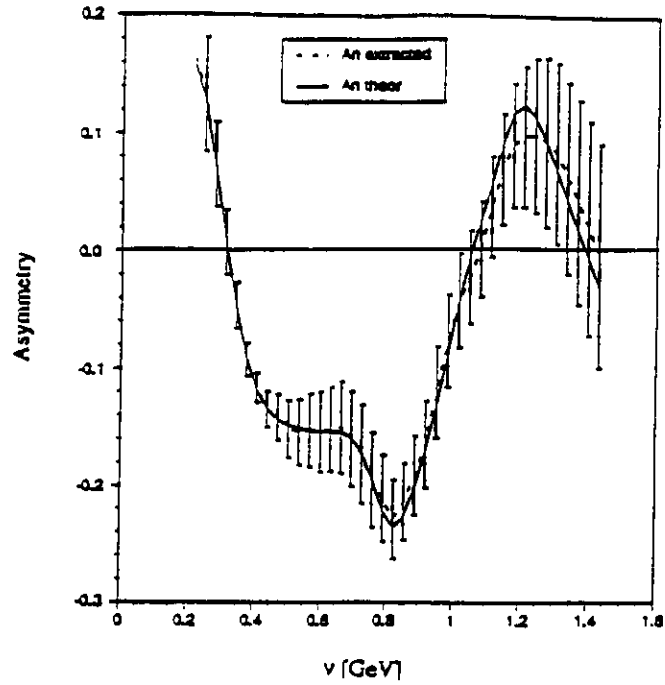


Figure 8: Expected statistical error for the asymmetry  $A/D(\epsilon x) \cdot \sigma_T$ . The deviations of the expected data points from the line indicate the systematic uncertainty due to the assumption  $A_2^{\pi} = 0$ .

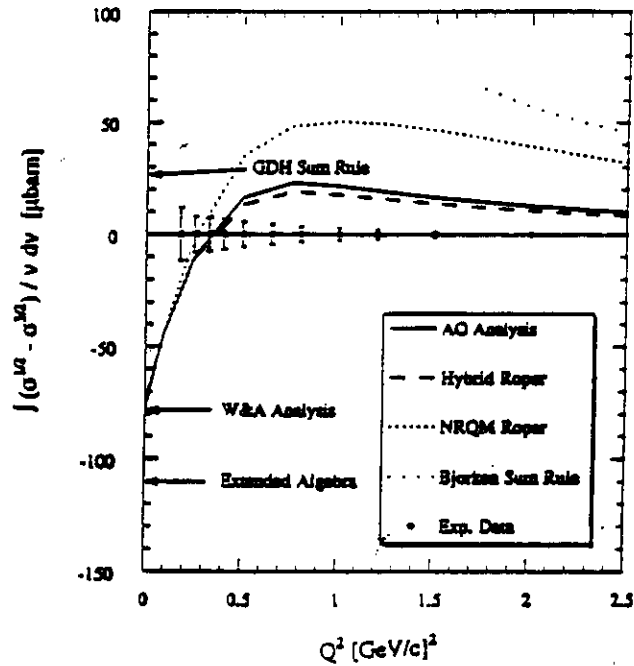


Figure 9: Expected errors for the proton - neutron difference  $\Delta I_{pn}(Q^2)$ .

$$\int A_1(\theta, \phi) P_1(\theta) \sin(\phi) d\Omega$$

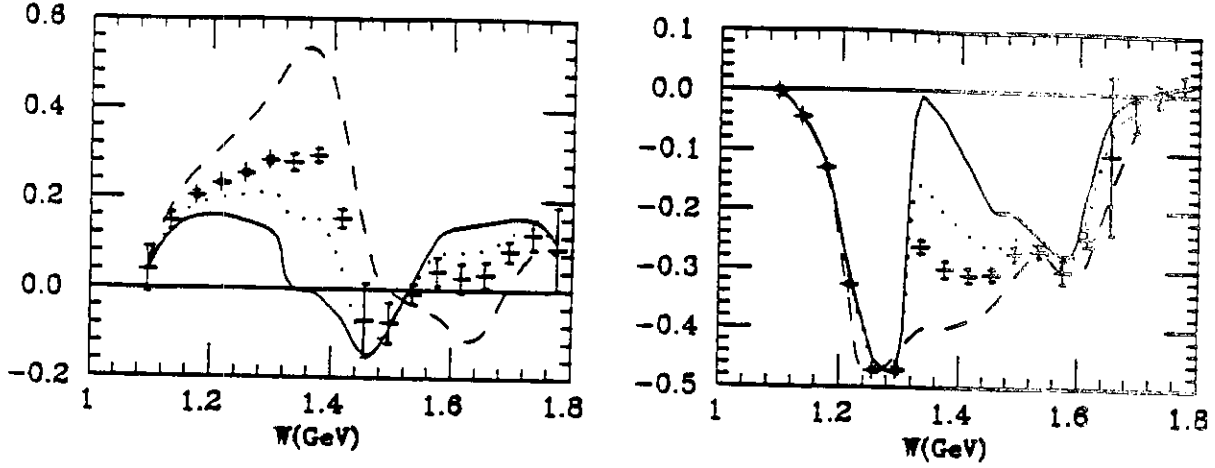


Figure 10: Moments of the polarized target asymmetry for single  $\pi^0$  (left) and  $\pi^+$  production. The curves represent results using the AO code<sup>19</sup> for various models of the  $P_{11}(1440)$  structure. Also shown are projected error bars for the experiment.

$$A_1^{res} = \frac{\sigma_{1/2}^T - \sigma_{3/2}^T}{\sigma_{1/2}^T + \sigma_{3/2}^T} = \frac{A_{1/2}^2 - A_{3/2}^2}{A_{1/2}^2 + A_{3/2}^2} \quad (12)$$

for these states. It will therefore be possible to determine the contributions of individual states to the GDH integral. In comparison with quark model calculations information about the QCD structure of the  $N^*$  and  $\Delta^*$  resonances will be obtained.

## 6. Summary

Measurement of polarized structure functions of the proton and neutron probe significant contributions to the spin integrals at low  $Q^2$  and  $\nu$  and are important for testing the validity of the GDH sum rule and models describing its extension to finite  $Q^2$ . Phenomenological analyses of pion photo- and electroproduction yield significant discrepancies with the GDH sum rule for the proton/neutron difference. The measurements will also provide tests of models of the nucleon structure. The measurements may have a bearing on the interpretation of the deep inelastic polarized structure functions at finite values of  $Q^2$ .

## References

1. J. Ashman et al., *Phys. Lett. B*206 (1988)364; *Nucl. Phys.*B328 (1989)1.
2. B. Adeva et al., *Phys. Lett. B* 302 533 (1993).
3. P.L. Anthony et al., *Phys. Rev. Lett.* (1993).
4. J.D. Björken, *Phys.Rev.*148, 1467(1966).
5. J. Ellis and R.L. Jaffe, *Phys. Rev. D*9, 1444 (1974)
6. G. Altarelli, G.G. Ross, *Phys. Lett. B*214, 381(1988); R. Carlitz, J.C. Collins, A.M. Mueller. *Phys. Lett.*B214, 2229 (1988)
7. R. Manohar. in: *Polarized Collider Workshop*, University Park, Pa. , 1990., AIP Conference Proc. No.223.
8. S. Gerasimov, *Yad.Fiz.*2, 598(1965) [*Sov. J. Nucl. Phys.*2 (1966)930].
9. S.D. Drell and A.C. Hearn, *Phys. Rev. Lett.* 16 (1966) 908.
10. I. Karliner, *Phys.Rev. D*7, 2717 (1973)
11. R. Workman and R. Arndt, *Phys. Rev. D*45, 1789(1992)
12. V. Burkert and Zh. Li, *Phys. Rev.*D47, 46(1993)
13. V. Burkert and Zh. Li, in preparation.
14. M. Anselmino, B.L. Ioffe and E. Leader, *Sov. J. Nucl. Phys.* 49 (1989) 136.
15. V. Burkert and B.L. Ioffe, *Phys. Lett.*B296 (1992)223
16. V. Burkert and B.L. Ioffe, Preprint CEBAF PR-93-034.
17. I.G. Aznauryan, *Yad. Fiz.* 6, 124(1966) [*Sov. J. Nucl. Phys.* 6, 91(1967)];
18. Z.P. Li, *Phys.Rev.*D47, 1854(1993)
19. V. Burkert and Zh. Li, Computer code AO (unpublished).
20. Z.P. Li, V. Burkert, Zh. Li, *Phys. Rev. D*46, 70(1992).
21. L.N. Chang, Y.G. Liang and R. Workman, (unpublished)
22. V. Burkert, D. Crabb, R. Minehart et al., *CEBAF Proposal* 91-023.
23. G. Baum et al., *Phys.Rev. Lett.* 45, 2000 (1980).
24. V. Burkert and B. Mecking, in: 'Modern Topics in Electron Scattering', in: *World Scientific*, 1991; eds. B. Frois and I. Sick.
25. S. Kuhn et al., *CEBAF Proposal* 93-009.
26. H. Weller, R. Chasteler and R. Minehart et al., *CEBAF proposal* 93-036.
27. CEBAF N\* program; *Proposals* 89-037, -038, -039, -040, -042, -043, 91-024, 93-06.
28. D. Drechsel and M. Giannini, Preprint MKPH-T-93-12.
29. S. Capstick, *Phys. Rev. D*46, 2864(1992)
30. J. Soifer and O. Teryaev, *Phys. Rev. Lett.* 70, 3373 (1993)
31. V. Bernard et al., *Phys. Rev. D*48, 3062 (1993)